Supplemental Information

Celastrol-induced Nur77 interaction with TRAF2 alleviates inflammation by promoting mitochondrial ubiquitination and autophagy

Mengjie Hu, Qiang Luo, Gulimiran Alitongbieke, Chenting Xu, Lei Xie, Xiaohui Chen, Duo Zhang, Yuqi Zhou, Zhaokai Wang, Xiaohong Ye, Lijun Cai, Fang Zhang, Huibin Chen, Fuquan Jiang, Hui Fang, Shanjun Yang, Jie Liu, Maria T Diaz-Meco, Ying Su, Hu Zhou, Jorge Moscat, Xiangzhi Lin, and Xiao-kun Zhang

Supplemental Experimental Procedures

Cell lines

Human hepatocellular carcinoma cell lines HepG2, SMMC-7721, QGY-7703 were maintained in Dulbecco's Modified Eagle Medium containing 10% fetal bovine serum (FBS). Human hepatocellular carcinoma cell line LO2, human lung carcinoma cell line NIH-H460 and human cervical cancer cell line HeLa were cultured in RPMI-1640 supplemented 10% FBS. Primary MEFs and Nur77$^{-/-}$ MEFs were extracted from fetus of 14d-16d wild-type and Nur77$^{-/-}$ pregnant female mice (C57BL/6 background).

Compounds

136 natural compounds with approved anti-inflammatory effect in human were purified from traditional Chinese medicinal plants and used to screen for binding to Nur77. Celastrol was obtained from *Thunder of God Vine*. The 60% aqueous ethanol (V/V) solution-soluble extract of *Thunder of God Vine* was extracted with ethyl acetate and the ethyl acetate fraction was separately subjected multiple chromatographic steps on silica gel or Sephadex LH-20. The subfraction was purified through preparative HPLC eluting with aqueous acetonitrile elution to produce celastrol. Celastrol purchased from Sigma (St. Louis, MO, USA) and Chengdu Pufei De Biotech Co., Ltd (Chengdu, Sichuan, China) was used to confirm the results.

Plasmids

Plasmids pcmv-myc-Nur77, pcmv-myc-Nur77/L506W, pcmv-myc-Nur77/L555W, pcmv-myc-Nur77/L556W, pcmv-myc-Nur77ΔAF2, pcmv-myc-Nur77ΔAB, pcmv-myc-Nur77ΔDBD, pcmv-myc-Nur77ΔAB/ΔDBD, pcmv-myc-Nur77ΔLBD, pEGFP-C1-Nur77, pET-15b-Nur77/LBD, pFlag-cmv-2-TRAF2, pFlag-cmv-2-TRAF3, pFlag-cmv-2-TRAF5, pFlag-cmv-2-TRAF2(1-249), pFlag-cmv-2-TRAF2(97-356), pFlag-cmv-2-TRAF2(272-501), GST-TRAF2, GFP-LC3, RFP-LC3, HA-Ub, HA-UbK63R, pBind-Nur77, pBind-GR/LBD, pG5pFlag-cmv-2-p62, Myc-Nur77/K536R, and GFP-Nur77/K536R were described previously (*1-5*) or were constructed using PCR or the QuikChange mutagenesis kit.

Antibody and reagents

Anti-Myc (9E10) (Cat. ab32), and anti-Hsp60 (Cat. ab46798) antibodies from Abcam (UK); anti-Ubiquitin (Cat. 3933S), anti-β-actin (Cat. 4970S), anti-IκBα (Cat.4814S), and anti-LC3 (Cat. 4108S) antibodies from Cell Signal Technology (Beverly, MA, USA); anti-Nur77 (M-210) (Cat. sc-5569), anti-LC3B (Santa Cruz sc-28266), anti-p65 (Santa Cruz sc-109) and anti-GST (Cat.sc-138) antibodies from Santa Cruz Biotechnology (Santa Cruz, CA, USA); mouse IL-1β (interleukin 1β, Cat. E-EL-M0037c) and IL-6 (interleukin 6, Cat. E-EL-M0044c) ELISA kits for IL-1β and IL6 from Elabscience Biotechnology (Wuhan, Hubei, China); LPS (Lipopolysaccharide, Cat. L2630) and D-Gal N (D-Galactosamine, Cat. G0500) from Sigma (St. Louis, MO, USA); TianScript RT kit (Cat. KR104-02) from TianGen Biotechnology (Beijing, China); and Nur77, RXRα, and control siRNAs from Sigma were used.

Real-time polymerase chain reaction (PCR)

After grinding liver tissue by tissuelyser-24, total RNA was extracted with Trizol. 2 μg total RNA was used to prepare cDNA using oligo(dT)12 as a primer. TIANScript RT Kit's was used for real-time PCR analysis. Each sample was run in triplicate. The relative RNA amounts were calculated with the ΔΔCt method

by ABI Stepone PCR instrument and normalized with an internal control, β-actin. Primers: IL-6 forward: CCAGAGATACAAAGAAATGATGG, reverse: ACTCCAGAAGACCAGAGGAAAT; IL-1β forward: TGGTGTGTGACGTTCCCATT, reverse: CAGCACGAGGCTTTTTTGTTG.

Biacore assay

After coupling 50 μg purified ligand-binding domain (LBD) of Nur77 (Nur77-LBD) protein to CM5 of Biacore, over one hundred compounds (20 μM) with known anti-inflammatory activity were initially screened for their binding to Nur77-LBD by Biacore T200. The identified celastrol was tested again with a gradient concentration of 0.04 μM, 0.08 μM, 0.16 μM, 0.32 μM, and 0.64 μM injected through flow cells immobilized with Nur77-LBD. The kinetic profiles were shown.

Circular dichroism (CD)

CD analysis of celastrol binding to Nur77-LBD followed protocol described previously (*2*). Celastrol (200 μl, 0.1 mg/ml) was added to the phosphate buffer (10 mM, pH7.4) of purified Nur77-LBD protein (1 ml, 1 mg/ml) extracted and purified from E. coli. After incubation for 3 hr at 4^{o}C, 0.7 mL of the incubation buffer was measured with Jasco J-810 spectropolarimeter, and the CD spectra were obtained from 190 nm to 260 nm. Nur77-LBD alone was used as control.

High performance liquid chromatography (HPLC). HPLC was conducted as described (*5*). Briefly, celastrol (600 μl, 0.1 mg/ml) was incubated with purified Nur77-LBD protein (5 ml, 1 mg/ml). After incubation for 3 hr at 4^{o}C, the complex of celastrol and Nur77-LBD was captured using Ni beads. The complex was degenerated and the bound celastrol was extracted by organic solvent. The bound celastrol was subjected to ODS column (5 μm, 4.6×250 mm) through 0.2% H_3PO_4 aqueous acetonitrile elution using HPLC spectrometer (Shimadzu LC 20A, Japan). The detection wavelength was 425 nm.

Molecular Simulation

Docking of celastrol to Nur77 (PDB code: 4JGV) was performed using AutoDock V4.2. as described (*5*). Celastrol conformations were generated by the Lamarckian genetic algorithm. Grid center was chosen around the reported coordinates (-12.08, 18.29, -4.233) of THPN in Nur77 crystal structure and grid size was set to 40x40x40 (X, Y, Z) grid points with a spacing of 0.375A between grid points. The standard docking protocol in AutoDock was applied: the number of randomly placed individuals was 150, the maximum number of energy evaluations was 2.5 million, the rate of gene mutation was 0.02, the rate of crossover was 0.8, the probability of performing local search on individual was 0.06, the lower bound on rho was 0.01. PyMOL version 0.99 was used for molecular visualization.

Dual-Luciferase Reporter Assay

Reporter assays were conducted as described (*1, 6, 7*). Cells were transfected with the corresponding plasmids for 24 hr and then treated with compounds for 12 hr. Cells were lysed and Lusiferase relative activity was tested by the Dual-Luciferase Reporter Assay System according to the manufacturer's instructions. Transfection efficiency was normalized to Renilla luciferase activity.

Confocal Microscopy

Confocal microscopy was conducted as described (*2-4*). Cells mounted on glass slides were permeabilized with PBS containing 0.1% TritonX-100 and 0.1 mol/L glycine for 15 min, and blocked with 1% bovine serum in PBS for 30 min at room temperature, followed with incubation with various primary antibodies at room temperature for 3 hr, and detected by FITC-labeled anti-IgG (1:400), anti-goat IgG conjugated with Cy3(1:400), or Cy5-labeled antibody at room temperature for 1 hr. Cells were costained with 4′,6-diamidino-2-phenylindole (DAPI) (1:10000 dilution) to visualize nuclei. The images were taken under a fluorescent microscope (CarlZeiss) or an LSM-510 confocal laser scanning microscope system (CarlZeiss). HepG2 cells, MEFs, and Nur77$^{-/-}$ MEFs were treated with celastrol (1 μM or 4 μM) for the indicated time before exposed to TNFα (20 ng/mL) for additional 30 min. Mitochondria were marked by Mitotracker (Red) (1:10000 dilution) for 30 min before fixed by 4% buffered formalin/PBS. Hsp60, Ub, p65, TRAF2, and Nur77 were examined by immunostaining.

Co-immunoprecipitation (co-IP)

Co-IP assays were conducted as described before (*2, 4, 5*). Cells were harvested in lysis buffer (10 mM Tris [pH 7.4], 150 mM NaCl, 1% Triton X-100, 5 mM ethylenediaminetetraacetic acid, containing protease inhibitors). Lysate was incubated with 1 μg antibody at 4°C for 2 hr. Immunocomplexes were then precipitated with 30 μl of protein A/G-sepharose. After an extensive washing with lysis buffer, the beads were boiled in SDS sample loading buffer and assessed by Western blotting (WB). HepG2 cells transfected with 2 μg Myc-Nur77, Flag-TRAF2, or HA-Ub expression vectors in 10-cm dishes were treated with treated with celastrol (4 μM) for 2 hr plus TNFα (20 ng/mL) for additional 30 min as indicated and analyzed by co-IP using anti-Myc or anti-Flag antibody.

Western blotting (WB)

WB was performed as described previously (*2, 4, 5*). Cell lysates were boiled in sodium dodecyl sulfate (SDS) sample loading buffer, resolved by 10% SDS–polyacrylamide gel electrophoresis (SDS–PAGE) and transferred to nitrocellulose. The membranes were blocked in 5% milk in Tris-buffered saline and Tween 20 (TBST; 10 mM Tris–HCl [pH 8.0], 150 mM NaCl, 0.05% Tween 20) for 1 hr at room temperature. After washing twice with TBST, the membranes were incubated with appropriate primary antibodies in TBST for 1 hr and then washed twice, probed with horseradish peroxide-linked anti-immunoglobulin (1:5000 dilution) for 1 hr at room temperature. After three washes with TBST, immunoreactive products were visualized using enhanced chemiluminescence reagents and autoradiography. HepG2 cells, MEFs and Nur77$^{-/-}$ MEFs were treated with Celastrol in 1 μM and 4 μM for 1 hr before exposed to TNFα (20 ng/mL) for additional 30 min. Lysates prepared were analyzed with IκB (1:1000 dilution) and β-actin (1:10000 dilution) antibodies by Western blotting. HepG2 cells, MEFs and Nur77$^{-/-}$ MEFs were treated with celastrol in 2 μM for 9 hr before exposed to TNFα (20 ng/mL) for additional 30 min. Lysates prepared were analyzed with LC3B (1:1000 dilution) and β-actin antibodies by Western blotting.

Animal studies

Wild-type and Nur77$^{-/-}$ mice (C57BL/6 background) were purchased from the Jackson Laboratory (Bar Harbor, Maine, USA). All of the mice were maintained in animal room with 12-hours light/12-hours dark cycles at Laboratory Animal Center in Xiamen University. Celastrol was dissolved in DMSO and diluted with normal saline containing 5.0% (V/V) Tween-80 to a final concentration 0.05 mg/mL. Normal saline with DMSO and 5.0% Tween-80 was employed as the vehicle control. For acute liver inflammation animal studies, mice of 8-10 weeks were intraperitoneally (i.p.) coinjected with LPS (80 μg/kg) and D-GalN (200 mg/kg). After 6 hr, mice were bled

from the eye and the concentrations of AST, ALT, IL-1β and IL-6 in blood were measured by ELISA assay. Liver tissues were also collected, and the relative levels of mRNA expression of IL-1β and IL-6 were determined by RT-PCR. To estimate the efficacy of celastrol, mice were intraperitoneally injected with celastrol (0.2 or 0.5 mg/kg body weight) 12 hr before LPS/D-GalN injection. For HFD-induced obese animal studies, wild-type and Nur77$^{-/-}$ lean male mice were placed on 60 kcal% HFD (research diet) at the age of four weeks soon after weaning, and maintained on the same diet for 17 weeks before the experiments. All other animals were maintained on chow diet (13.5% from fat calories; lab diet). Animals were housed under 12 hr of light and 12 hr dark cycle with unrestricted access to food and water unless otherwise described. Vehicle or Celastrol (0.1 mg/kg) was administered at fixed time (7:00 PM) once a day for two weeks (i.p., once a day). Body weight was monitored daily before drug treatment.

Mouse tissue processing and histological examination

Mouse tissues for histological examination were fixed in 10% or 4% neutral buffered formalin phosphate (pH 7.0) for periods not exceeding 24 hr, and were subsequently embedded in paraffin or OCT compound, respectively. They were sliced into 4-μm sections for hematoxylin and eosin (HE) staining, immunofluorescence, and for immunohistochemistry. To examine hepatocytes, HE-stained liver sections were analyzed with an image analysis system (Olympus, Tokyo, Japan)**.** For immunostaining, liver sections were incubated with anti-LC3B (1:150 dilution) or anti-p65 (1:100 dilution) antibody. Positive areas were counted and measured, respectively, for 10 low-powered (×100) fields per slide and analyzed by ImageJ software (NIH). A total of 10 sections in ablation region, each section randomly selected five fields at x400 magnification and photographed counting the number of cells. The cells of sections independently counted and analyzed by GrapgPad Prism by two pathologists previously uninformed.

Detection of AST, ALT, IL-1β, and IL-6 Levels from Serum

Serum levels of liver enzymes, including AST and ALT, were determined using an automatic analyzer (NanJingjiancheng, China). Serum levels of IL-1β and IL-6 were determined by enzyme-linked immunosorbent assays (ELISA) according the manufacturer's protocol (Elabscience, China).

Prediction of potential ubiquitination sites on Nur77

Several online programs including UbPred, CPLM 1.0, and BDM-PUB were used to predict potential ubiquitination sites on Nur77. Three sites (Lys32, Lys381, and Lys536) were predicted to be potential ubiquitination sites on Nur77 and were there chosen for mutagenesis studies.

Statistical analyses

ANOVA with Tukey's post-test (One-way ANOVA for comparisons between groups, Two-way ANOVA for comparisons of magnitude of changes between different groups from different cell lines) was used to compare values among different experimental groups using the GraphPad program. For experiments with only two groups, Student's t-test was used as specified in the figure legends. $P<0.05$ was considered statistically significant (*), $P<0.01$ as highly significant (**), $P<0.001$ as extremely significant (***), and ns as not significant.

Supplemental References

1. L. Chen *et al.*, Sulindac-derived RXRalpha modulators inhibit cancer cell growth by binding to a novel site. *Chemistry & biology* **21**, 596-607 (2014).
2. S. K. Kolluri *et al.*, A short Nur77-derived peptide converts Bcl-2 from a protector to a killer. *Cancer cell* **14**, 285-298 (2008).
3. H. Li *et al.*, Cytochrome c release and apoptosis induced by mitochondrial targeting of nuclear orphan receptor TR3 [see comments] [comment]. *Science* **289**, 1159-1164 (2000).
4. B. Lin, Kolluri, S., Lin, F., Liu, W., Han, Y.H., Cao, X., Dawson, M.I., Reed, J.C., and Zhang, X.K., Conversion of Bcl-2 from Protector to Killer by Interaction with Nuclear Orphan Receptor Nur77/TR3. *Cell* **116**, 527-540 (2004).
5. H. Zhou *et al.*, NSAID sulindac and its analog bind RXRalpha and inhibit RXRalpha-dependent AKT signaling. *Cancer cell* **17**, 560-573 (2010).
6. G. H. Wang *et al.*, Targeting truncated retinoid X receptor-alpha by CF31 induces TNF-alpha-dependent apoptosis. *Cancer research* **73**, 307-318 (2013).
7. Z. Zeng *et al.*, Nitrostyrene Derivatives Act as RXRalpha Ligands to Inhibit TNFalpha Activation of NF-kappaB. *Cancer research* **75**, 2049-2060 (2015).

Figure S1

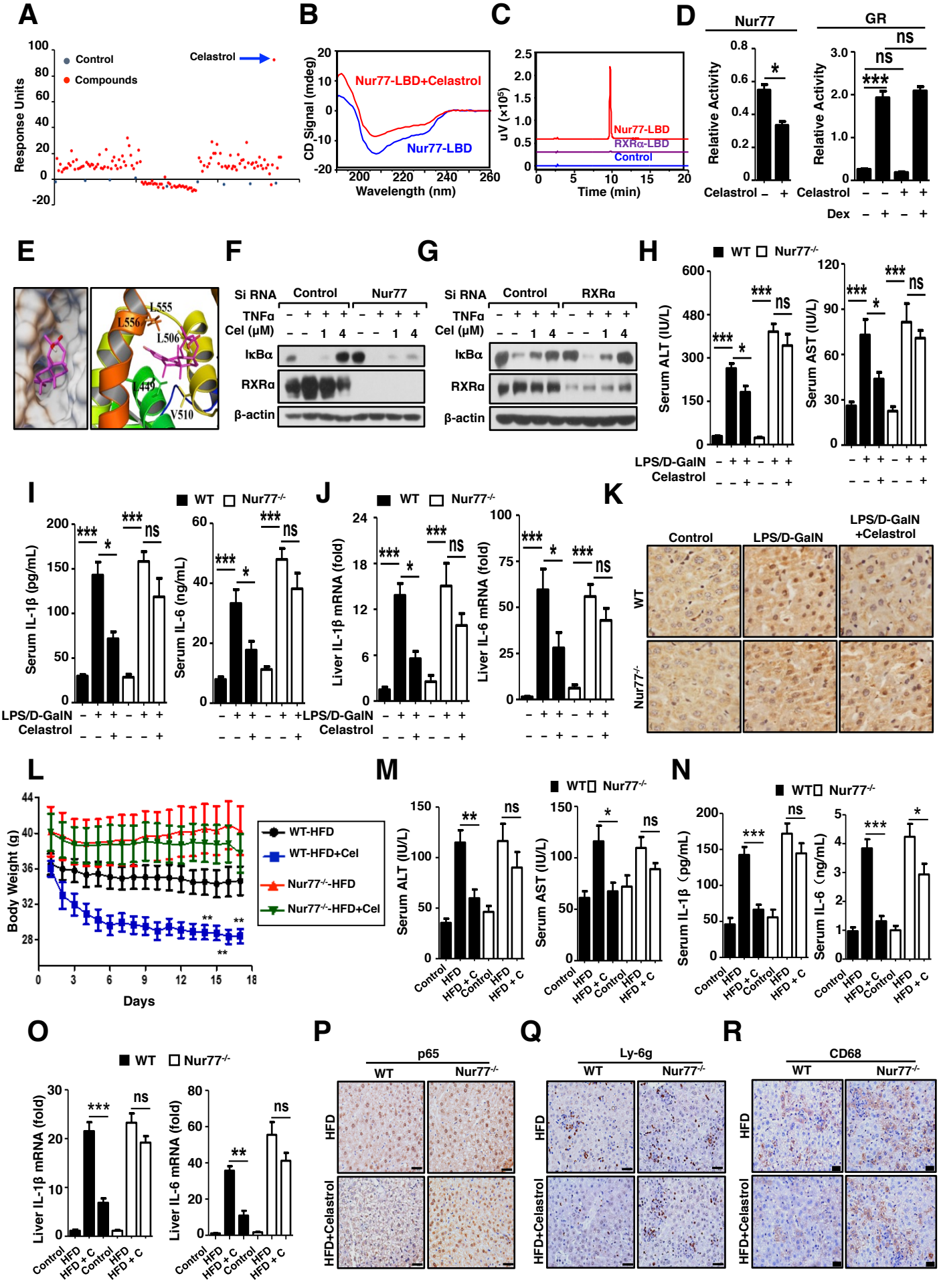
A
Response Units
Control
Compounds
Celastrol
B
CD Signal (mdeg)
Nur77-LBD+Celastrol
Nur77-LBD
Wavelength (nm)
C
uV (×10⁵)
Nur77-LBD
RXRα-LBD
Control
Time (min)
D
Nur77
GR
Relative Activity
Celastrol
Dex
E
L555
L556
L506
L449
V510
F
Si RNA
Control
Nur77
TNFα
Cel (μM)
IκBα
RXRα
β-actin
G
Si RNA
Control
RXRα
TNFα
Cel (μM)
IκBα
RXRα
β-actin
H
WT
Nur77-/-
Serum ALT (IU/L)
Serum AST (IU/L)
LPS/D-GalN
Celastrol
I
WT
Nur77-/-
Serum IL-1β (pg/mL)
Serum IL-6 (ng/mL)
LPS/D-GalN
Celastrol
J
WT
Nur77-/-
Liver IL-1β mRNA (fold)
Liver IL-6 mRNA (fold)
LPS/D-GalN
Celastrol
K
Control
LPS/D-GalN
LPS/D-GalN +Celastrol
WT
Nur77-/-
L
Body Weight (g)
Days
WT-HFD
WT-HFD+Cel
Nur77-/--HFD
Nur77-/--HFD+Cel
M
WT
Nur77-/-
Serum ALT (IU/L)
Serum AST (IU/L)
Control
HFD
HFD + C
N
WT
Nur77-/-
Serum IL-1β（pg/mL)
Serum IL-6（ng/mL)
O
WT
Nur77-/-
Liver IL-1β mRNA (fold)
Liver IL-6 mRNA (fold)
P
p65
WT
Nur77-/-
HFD
HFD+Celastrol
Q
Ly-6g
WT
Nur77-/-
HFD
HFD+Celastrol
R
CD68
WT
Nur77-/-
HFD
HFD+Celastrol

Figure S1. **Celastrol binding to Nur77 and regulation of inflammation,** ***related to Figure 1.***

(**A**) Identification of celastrol as a potent Nur77 binder. Representative SPR screen over one hundred anti-inflammatory natural products derived from from marine and terrestrial sources for binding the purified ligand-binding domain of Nur77 (Nur77-LBD) by Biacore T200. Some marine and terrestrial compounds, including celastrol indicated by arrow, were found to bind Nur77.

(**B**) Celastrol binding to Nur77 was demonstrated by altered CD spectra of purified Nur77-LBD by celastrol.

(**C**) HPLC analysis demonstrates binding of celastrol to the purified Nur77-LBD but not RXRα-LBD.

(**D**) Celastrol inhibits transactivation of Nur77 but not GR. Effect of celastrol (0.5 μM) on constitutive Nur77 or dexamethasone (Dex) (10^{-7} M)-induced GR transactivation was analyzed in HEK-293T cells by reporter assay. Data represent means ± SEM. *P< 0.05, **P< 0.01, ***P< 0.001 (Student's t test). ns, not significant.

(**E**) Computer-assisted analysis of celastrol binding to Nur77. Docked conformation of celastrol (in fuchsia) in Nur77-LBD (PDB ID: 4JGV).

(**F,G**) Knocking down Nur77 but not RXRα attenuates the anti-inflammatory effect of celastrol. HepG2 cells transfected with Nur77 siRNA (**F**), RXRα siRNA (**G**), or control siRNA were treated with celastrol for 1 hr before exposed to TNFα (20 ng/mL) for 30 min, and analyzed by Western blotting (WB). One of three similar experiments is shown.

(**H**) Inhibitory effect of celastrol on serum production of ALT and AST. The results showed that celastrol is much more effective in inhibiting the production of ALT and AST in wild-type mice than in $Nur77^{-/-}$ mice.

(**I**) Inhibitory effect of celastrol on serum production of IL-1β and IL-6. The results showed that celastrol is much more effective in inhibiting the production of IL-1β and IL-6 in wild-type mice than in $Nur77^{-/-}$ mice.

(**J**) Role of Nur77 in celastrol inhibition of LPS-D-GalN-induced IL-1β and IL-6 expression. Effect of celastrol on mRNA expression of IL-1β and IL-6 in liver of wild-type and $Nur77^{-/-}$ mice intraperitoneally (i.p.) injected with 80 μg/kg LPS and 200 μg/kg D-GalN for 6 hr and treated with or without celastrol (0.5 mg/kg) for 12 hr. n≥6.

(**K**) Role of Nur77 in celastrol inhibition of LPS-D-GalN-induced p65 nuclear translocation. Representative images of immunohistochemistry staining of p65 of liver tissues (scale bar, 20 μm).

(**L**) Nur77 deficient attenuates the anti-obesity effect of celastrol. Body weight in HFD-induced obesity mice during the treatment (n≥6 per group). Data represent mean ± SEM of three independent experiments. **P< 0.01 (Student's t test).

(**M**) Effect of celastrol on serum production of ALT and AST in HFD-induced mice. The data demonstrated that celastrol is more effective in inhibiting the production of ALT and AST in wild type mice than in $Nur77^{-/-}$ mice.

(**N**) Effect of celastrol on serum production of IL-1β and IL-6 in HFD-induced mice. The data demonstrated that celastrol is more effective in inhibiting the production of IL-1β and IL-6 in wild type mice than in $Nur77^{-/-}$ mice. n≥6, Data represent mean ± SEM of three independent experiments. ns, not significant, *P< 0.05, **P< 0.01, ***P< 0.001 (Student's t test).

(**O**) Role of Nur77 in celastrol inhibition of HFD-induced IL-1β and IL-6 expression. Effect of celastrol on mRNA expression of IL-1β and IL-6 in liver of mice (n≥6 per group). Celastrol, C.

(**P**-**R**) Role of Nur77 in celastrol inhibition of HFD-induced inflammation. Representative images of immunohistochemistry staining for p65 (**P**), and immunohistochemistry staining for Ly-6g (**Q**) and CD68 (**R**) of liver tissue from wild-type and $Nur77^{-/-}$ mice fed with HFD (n≥6 per group). Scale bar, 50 μm.

All the bar graphs represent mean ± SEM of three independent experiments. ns, not significant, *P< 0.05, **P< 0.01, ***P< 0.001 (Student's t test).

Figure S2

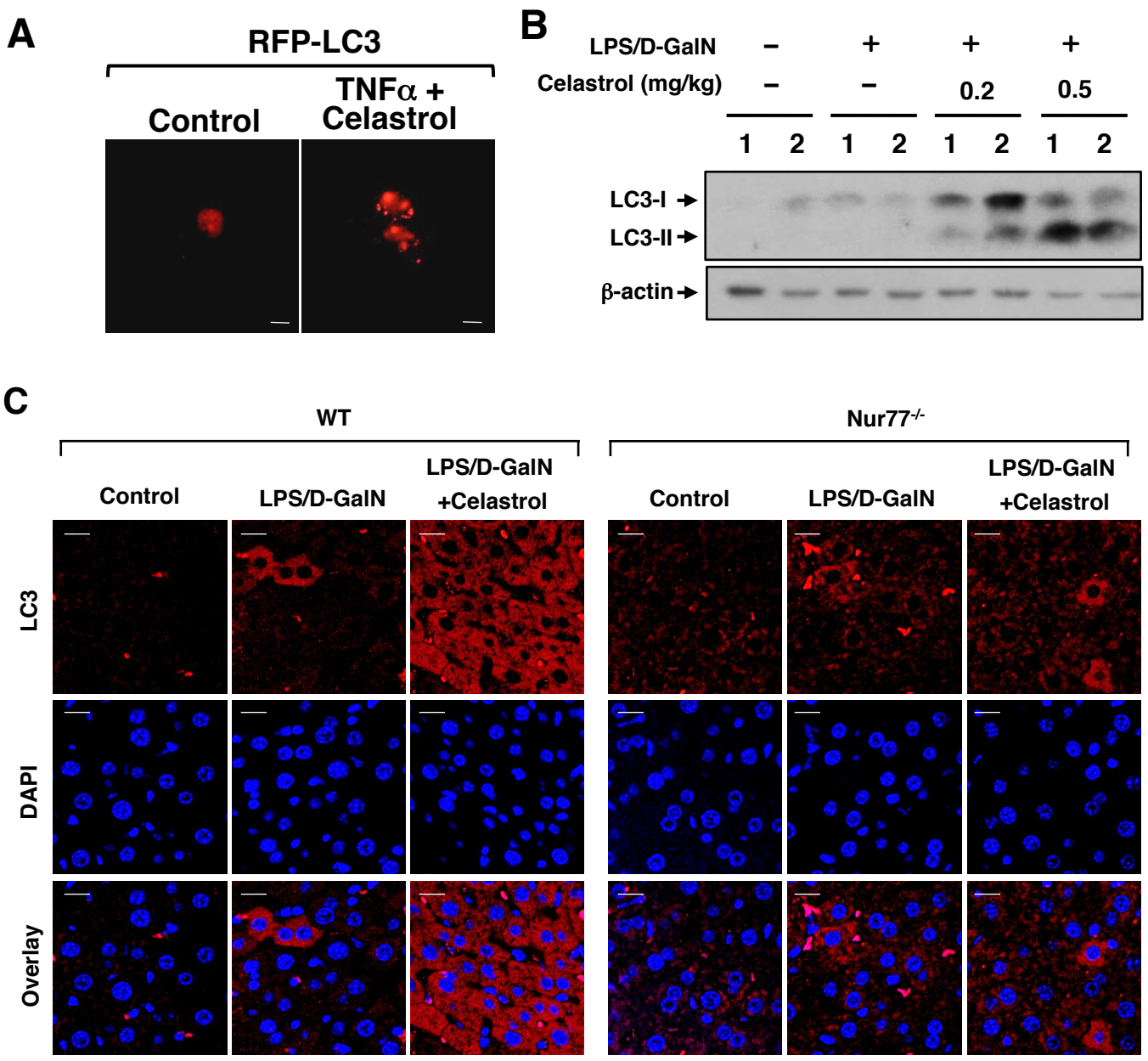

Figure S2. Related to Figure 2.

Nur77 is required for celastrol induction of autophagy.

(A) Celastrol induces autophagy. Representative images showing the formation of RFP-LC3 puncta in HepG2 cells after treatment with celastrol and TNFα for 3 hr. Scale bar, 10 μM.

(B) Induction of LC3-II expression by celastrol in mice injected with LPS/D-GalN. Lysates from liver tissues from two mice injected with LPS/D-GalN were analyzed by Western blotting for the expression of LC3-I and LC3-II. The results showed that celastrol strongly enhanced the level of LC3-II in liver tissues from LPS/D-GalN-injected mice in a dose dependent manner.

(C) Induction of autophagy by celastrol in mice injected with LPS/D-GalN is Nur77 dependent. Representative confocal images of immunofluorescence staining of liver tissue specimens from the indicated mice for LC3B (red) and DAPI (blue). Scale bar, 20 μM. The results showed that celastrol could strongly induce autophagy in wild type mice but not in Nur77$^{-/-}$ mice injected with LPS/D-GalN.

Figure S3

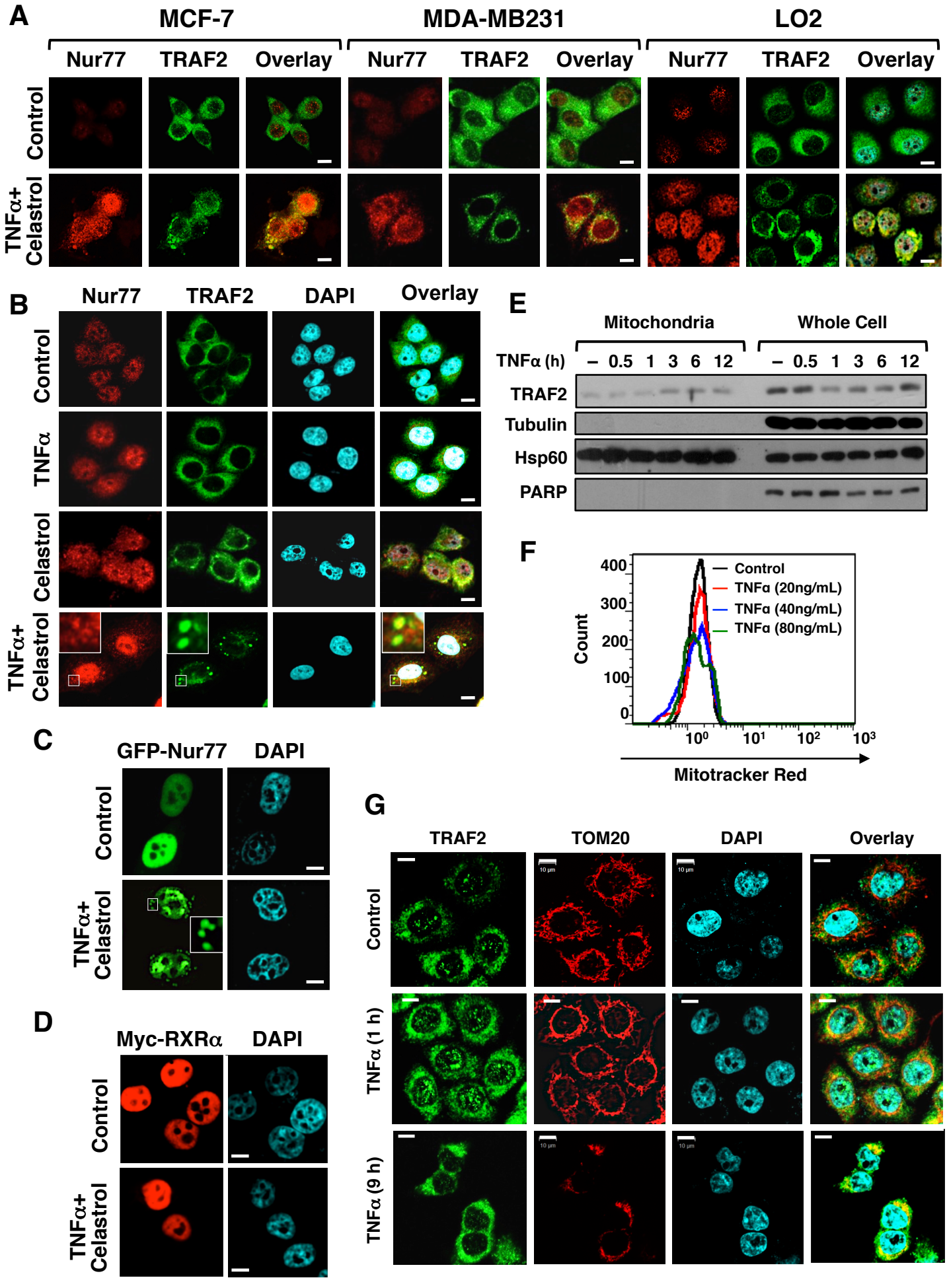
A
MCF-7
MDA-MB231
LO2
Nur77
TRAF2
Overlay
Control
TNFα+ Celastrol
B
Nur77
TRAF2
DAPI
Overlay
Control
TNFα
Celastrol
TNFα+ Celastrol
C
GFP-Nur77
DAPI
Control
TNFα+ Celastrol
D
Myc-RXRα
DAPI
Control
TNFα+ Celastrol
E
Mitochondria
Whole Cell
TNFα (h)
– 0.5 1 3 6 12
TRAF2
Tubulin
Hsp60
PARP
F
Control
TNFα (20ng/mL)
TNFα (40ng/mL)
TNFα (80ng/mL)
Count
400
300
200
100
0
10^0
10^1
10^2
10^3
Mitotracker Red
G
TRAF2
TOM20
DAPI
Overlay
Control
TNFα (1 h)
TNFα (9 h)

Figure S3

Figure S3. Related to Figure 3.

Celastrol promotes Nur77 colocalization with TRAF2 at mitochondria.

(A) Induction of Nur77 cytoplasmic localization by celastrol. The indicated cell lines were treated with or without 1 μM celastrol plus 20 ng/mL TNFα for 30 min were analyzed by immunofluorescence staining to reveal the subcellular localization of Nur77 and TRAF2. Scale bar 10 μm. The results demonstrate a potent effect of celastrol in inducing cytoplasmic localization of Nur77 in different cell types.

(B) Colocalization of endogenous Nur77 and TRAF2. Representative images showing colocalization of endogenous TRAF2 and Nur77 with mitochondria in HepG2 cells after treatment with celastrol (2 μM) and/or TNFα (20 ng/ml) for 1 hr, examined by immunostaining. Scale bar 10 μm.

(C, D) Celastrol induces cytoplasmic localization of GFP-Nur77 but not Myc-RXRα. HepG2 cells transfected with GFP-Nur77 (D) or Myc-RXRα (E) were treated with or without 1 μM celastrol plus 20 ng/mL TNFα for 1 hr, and analyzed by immunofluorescence staining. The data reveal a selective effect of celastrol. Scale bar 10 μm.

(E) TNFα promotes TRAF2 mitochondrial accumulation. Mitochondrial fractions and whole cell lysates prepared from HepG2 cells treated with TNFα (40 ng/ml) for the indicated time were analyzed by Western blotting. The results show that TNFα treatment could promote TRAF2 mitochondrial accumulation in a time dependent manner.

(F) Prolonged treatment of cells with TNFα results in loss of mitochondrial membrane potential. MitoTracker Red staining of mitochondria is sensitive to mitochondrial membrane potential. HepG2 cells treated with TNFα for 6 hr were stained with MitoTracker Red and analyzed by flow cytometry. The results showed a does dependent loss of mitochondrial membrane potential in cells treated with TNFα for 6 hr.

(G) Prolonged treatment of cells with TNFα results in collapse of mitochondrial network. HepG2 cells treated with TNFα (20 ng/mL) for 1 hr or 9 hr were examined for mitochondrial morphology by immunostaining TOM20, a mitochondrial outer membrane receptor. Scale bar, 10 μM. TOM20 staining demonstrated that a prolonged treatment of cells with TNFα resulted in collapse of mitochondrial network, likely reflecting their depolarization. Scale bar 10 μm.

Figure S4

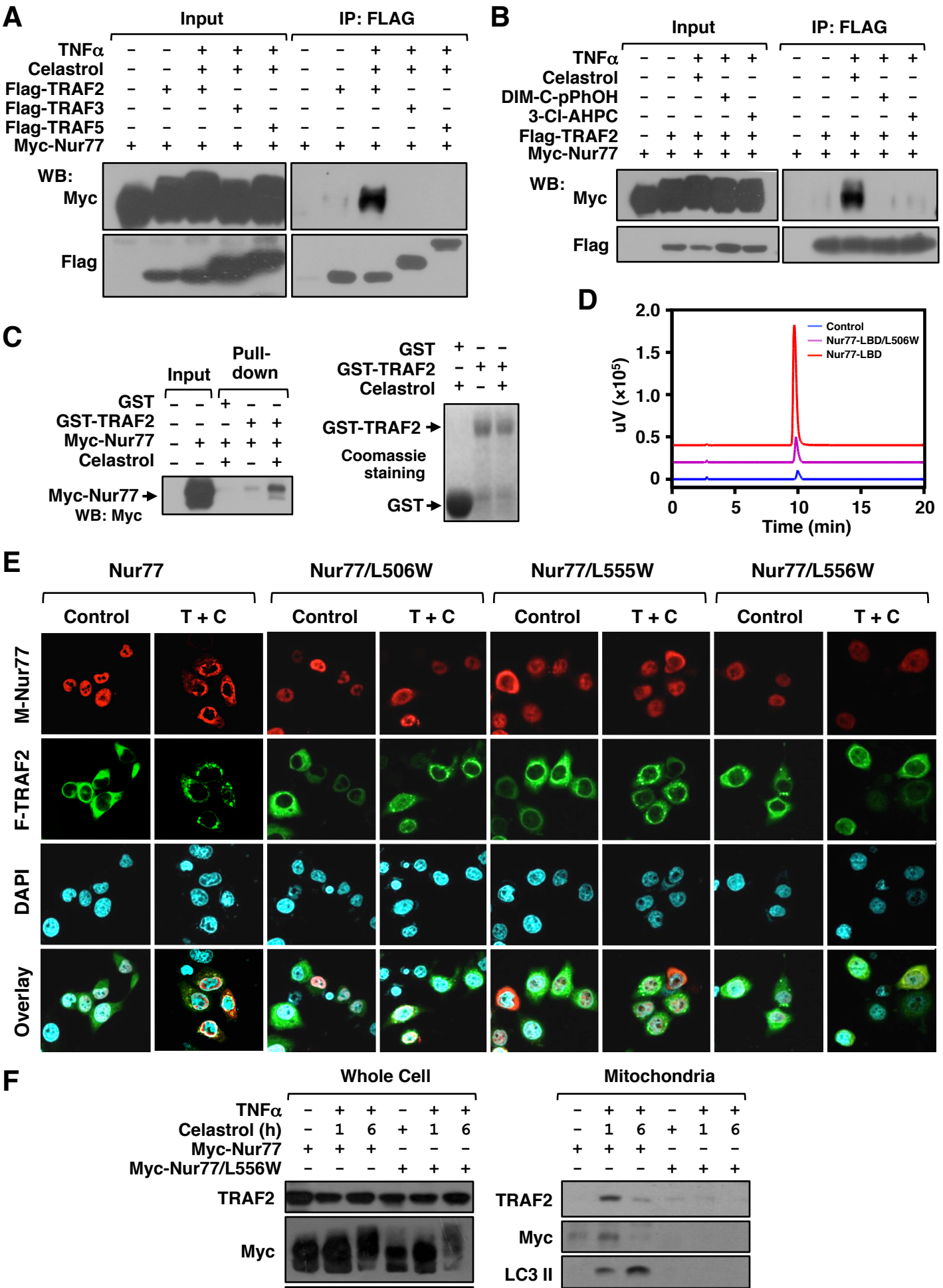
A
Input
IP: FLAG
TNFα
Celastrol
Flag-TRAF2
Flag-TRAF3
Flag-TRAF5
Myc-Nur77
WB:
Myc
Flag
B
Input
IP: FLAG
TNFα
Celastrol
DIM-C-pPhOH
3-Cl-AHPC
Flag-TRAF2
Myc-Nur77
WB:
Myc
Flag
C
Input
Pull-down
GST
GST-TRAF2
Myc-Nur77
Celastrol
Myc-Nur77
WB: Myc
GST
GST-TRAF2
Celastrol
GST-TRAF2
Coomassie staining
GST
D
Control
Nur77-LBD/L506W
Nur77-LBD
uV (×10⁵)
2.0
1.5
1.0
0.5
0
0
5
10
15
20
Time (min)
E
Nur77
Nur77/L506W
Nur77/L555W
Nur77/L556W
Control
T + C
M-Nur77
F-TRAF2
DAPI
Overlay
F
Whole Cell
Mitochondria
TNFα
Celastrol (h)
Myc-Nur77
Myc-Nur77/L556W
TRAF2
Myc
PARP
TRAF2
Myc
LC3 II
Hsp60

Figure S4

Figure S4. Related to Figure 4.

Celastrol induces Nur77 interaction with TRAF2.

(A) Selective effect of celastrol in promoting Nur77 interaction with TRAF2. Interaction of transfected Nur77 with the indicated TRAF2, TRAF3, or TRAF5 plasmid in HepG2 cells treated with TNFα (20 ng/ml) and celastrol (1 μM) was analyzed by co-IP.

(B) Selective effect of celastrol in promoting Nur77 interaction with TRAF2. Interaction of transfected Nur77 with TRAF2 in HepG2 cells treated with TNFα (20 ng/ml) and celastrol (1 μM), DIM-C-pPhOH (1 μM), or 3-Cl-AHPC (1 μM) was analyzed by co-IP.

(C) Celastrol induces Nur77 interaction with TRAF2 in vitro. Left panel: Purified bead-bound GST or GST-TRAF2 protein was incubated with celastrol (4 μM) and HepG2 cell lysates containing transfected myc-Nur77. After GST-pulling down and washing, reactions were analyzed by Western blotting. Right panel: Coomassie staining of GST and GST-Nur77 proteins used in GST-pull down experiments shown in right panel. The results showed that Myc-TRAF2 expressed in cells was specifically pulled down by GST-Nur77 protein but not by GST control protein in the presence of celastrol.

(D) HPLC analysis demonstrates binding of celastrol to the purified Nur77-LBD but not Nur77-LBD/L506W.

(E) Effect of celastrol on inducing colocalization of Flag-TRAF2 (F-TRAF2) and Myc-Nur77 (M-Nur77) mutants. HepG2 cells transfected with Flag-TRAF2 and the indicated Myc-Nur77 mutants were treated with celastrol (4 μM) and/or TNFα (20 ng/ml) for 1 hr. Colocalization of transfected Flag-TRAF2 and Myc-Nur77 mutants were examined by immunofluorescence staining. The results showed extensive colocalization of transfected Flag-TRAF2 with wild-type Nur77, whereas Flag-TRAF colocalization with Nur77/L506W, Nur77/L555W and Nur77L556W in the cytoplasm was largely impaired, when cells were cotreated with celastrol and TNFα. These results support our conclusion that binding of celastrol to Nur77 is critical for its induction of Nur77 interaction with TRAF2.

(F) Celastrol-induced Nur77 interaction with TRAF2 plays a role in TRAF2 mitochondrial localization and autophagy. Celastrol induces co-accumulation of TRAF2 with Nur77 but not Nur77/L556W at mitochondria, which correlated with its induction of LC3 II expression. Whole cell lysates and mitochondrial fractions prepared from HepG2 cells treated with celastrol (4 μM) and/or TNFα (20 ng/ml) were analyzed by Western blotting. One of two similar experiments is shown.

Figure S5

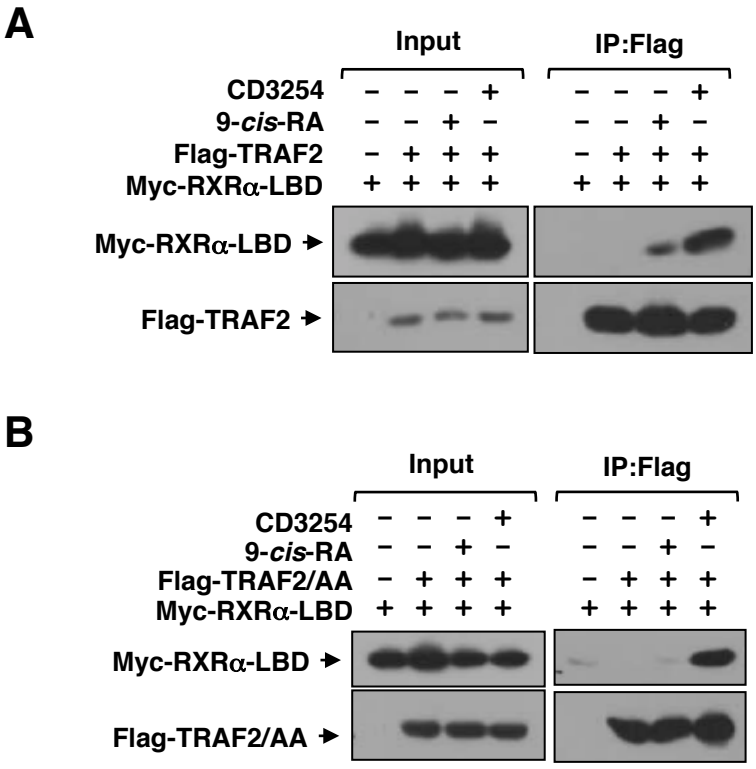

Figure S5. Related to Figure 5.
The role of "LAMLL" motif in 9-*cis*-RA-dependent interaction of TRAF2 with RXRα-LBD.
(A, B) Myc-RXRα-LBD was cotransfected into HepG2 cells together with Flag-TRAF2 (**A**) or Flag-TRAF2/AA (**B**). Cells were then treated with or without 9-*cis*-RA (10^{-7} M) or synthetic RXRα agonist CD5234 (10^{-7} M) (*PNAS* 104, 17323-17328, 2007) overnight. Interaction of RXRα-LBD with TRAF2 or TRAF2/AA was analyzed by co-IP assay using anti-Flag antibody. The results showed that 9-*cis*-RA was able to induce interaction of RXRα-LBD with TRAF2 but not TRAF2/AA, demonstrating the significance of the LAMLL motif in TRAF2 for 9-*cis*-RA modulation of RXRα-LBD with TRAF2. Interestingly, the strong induction of CD3254 on RXRα-LBD interaction with TRAF2 was not affected by the mutation of TRAF2-LXXLL motif, suggesting that other motifs may play a role.

Figure S6

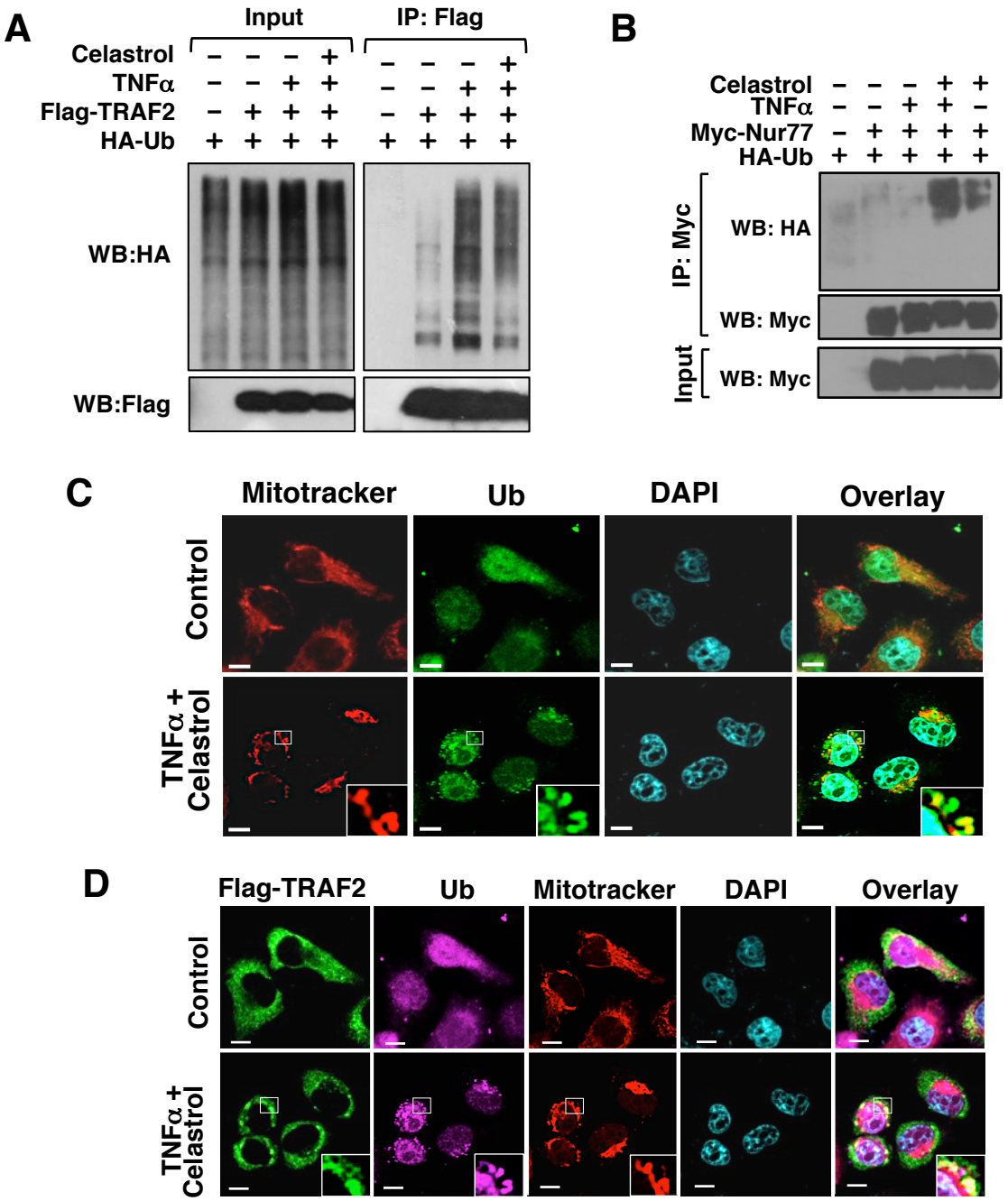

Figure S6. Related to Figure 6.

Role of celastrol induction of Nur77 ubiquitination in mitochondrial ubiquitination and autophagy.

(A) Inhibition of TRAF2 polyubiquitination by celastrol. HepG2 cells transfected with the indicated Flag-TRAF2 and HA-Ub were treated with 4 μM celastrol and/or 20 ng/ml TNFα for 1 hr, and analyzed by co-IP followed by Western blotting.

(B) Effect of celastrol and TNFα on Nur77 ubiquitination. HepG2 cells transfected with the indicated plasmids were treated with celastrol (4 μM) and TNFα (20 ng/ml) for 1 hr and analyzed by co-IP. The results showed that transfected Nur77 was heavily ubiquitinated when cells were treated with celastrol. Addition of TNFα enhanced the effect of celastrol on Nur77 ubiquitination.

(**C**) Celastrol promotes mitochondrial ubiquitination. Representative confocal microscopy images illustrating colocalization of mitochondria with Ub in HepG2 cells treated with celastrol/TNFα as above. Scale bar, 10 μm.

(D) Celastrol promotes TRAF2 colocalization with Ub at mitochondria. Representative images illustrating colocalization of transfected Flag-TRAF2 with Ub and mitochondria in HepG2 cells treated with celastrol/TNFα as above. Scale bar, 10 μm.

Figure S7

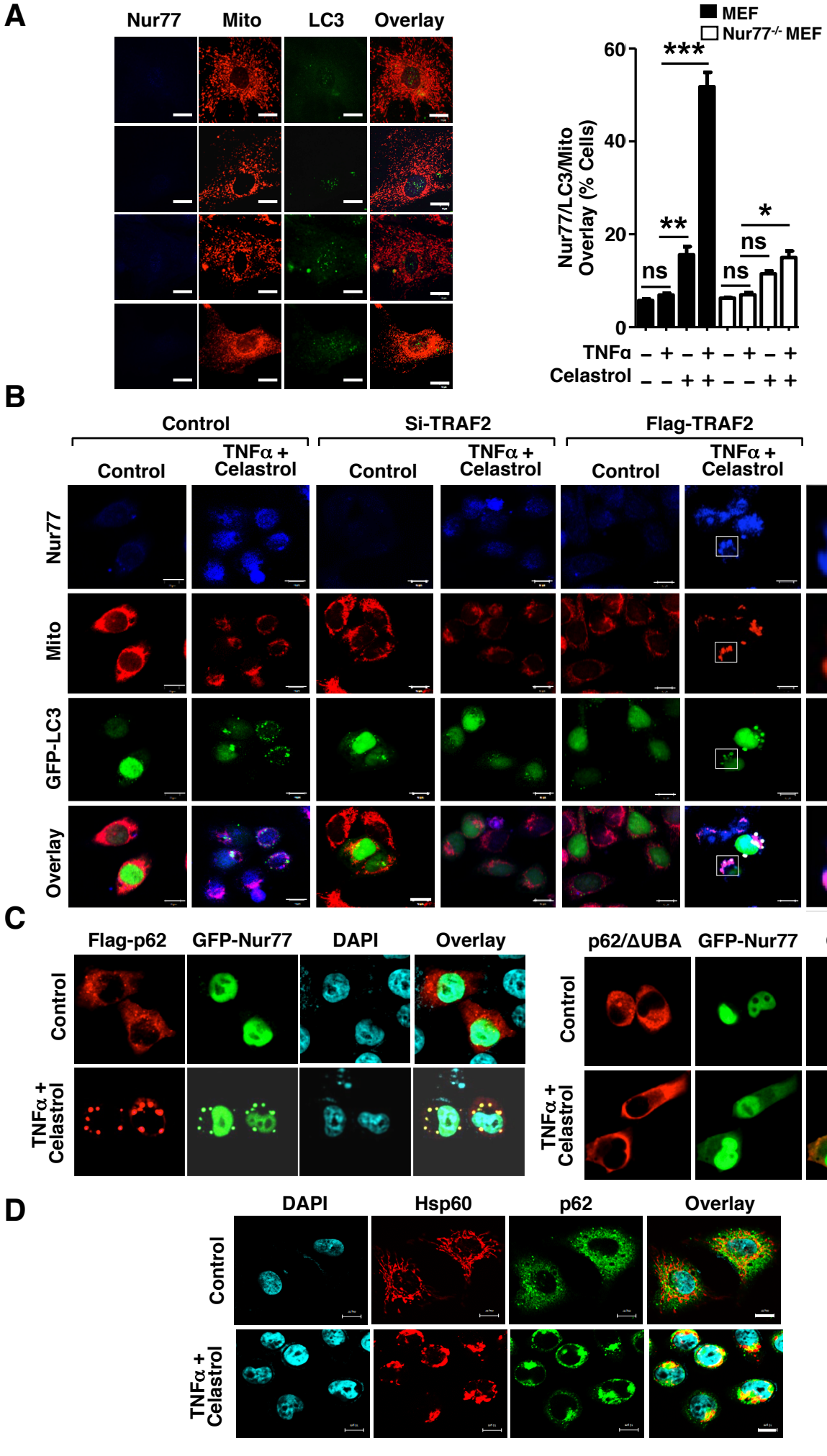
A
Nur77
Mito
LC3
Overlay
MEF
Nur77-/- MEF
Nur77/LC3/Mito Overlay (% Cells)
60
40
20
0
***
**
*
ns
ns
ns
TNFα – + – + – + – +
Celastrol – – + + – – + +
B
Control
Si-TRAF2
Flag-TRAF2
Control
TNFα + Celastrol
Control
TNFα + Celastrol
Control
TNFα + Celastrol
Boxed areas
Nur77
Mito
GFP-LC3
Overlay
C
Flag-p62
GFP-Nur77
DAPI
Overlay
Control
TNFα + Celastrol
p62/ΔUBA
GFP-Nur77
Overlay
Control
TNFα + Celastrol
D
DAPI
Hsp60
p62
Overlay
Control
TNFα + Celastrol

Figure S7. Related to Figure 7.

Celastrol induces interaction of mitochondrial Nur77 interaction with p62//SQSTM1 and mitophagy

(A) Celastrol fails to promotes LC3 colocalization with mitochondria in Nur77$^{-/-}$ MEFs. Representative images showing lack of colocalization of LC3 with mitochondria in Nur77$^{-/-}$ MEFs after treatment with celastrol (2 μM) and TNFα (20 ng/ml) for 1 hr, examined by immunostaining. Colocalization of endogenous Nur77 with mitochondria and LC3 in MEFs was illustrated in Figure 7A. Statistical data were mean ± SEM of 5 independent images including those shown in Figure 7A. ns, not significant, *P< 0.05, **P< 0.01, ***P< 0.001 (Student's t test).

(B) Celastrol-induced Nur77 colocalization with mitochondria and GFP-LC3 is TRAF2 dependent. Representative images illustrating the role of TRAF2 in the formation of Nur77 puncta and their colocalization with GFP-LC3 and mitochondria. HepG2 cells transfected with GFP-LC3 and TRAF2 siRNA or Flag-TRAF2 were treated with celastrol/TNFα as above. Scale bar, 20 μm.

(C) The ubiquitin-associated (UBA) domain in p62 is required for celastrol-TNFα-induced colocalization of p62 with Nur77. HepG2 cells transfected with GFP-Nur77 and Flag-p62 or Flag-p62/ΔUBA were treated with 4 μM celastrol and TNFα (20 ng/ml) for 1 h, and analyzed by immunostaining. The results showed that GFP-Nur77 colocalized extensively with Flag-p62 but not with Flag-p62/ΔUBA when cells were treated with celastrol and TNFα.

(D) Celastrol promotes p62 colocalization with mitochondria. HepG2 cells were treated with or without 4 μM celastrol and TNFα (20 ng/ml) for 1 h, and analyzed by immunostaining. The data showed that mitochondrial localization of p62 was significantly enhanced in cells treated with celastrol.

Scale bar, 10μm.